tallographically required to have a linear V–O–C–V moiety. A summary of C–O–M bond angles for structurally characterized carbonyl-bridged complexes reported in the literature may be found in Table VI. Examination of these data reveals the angles of 166 (1) and 177.8 (3)° for the M–O–C bond in **3b** and **4**, respectively, to be two of the most nearly linear bridged carbonyl complexes to have been structurally characterized.

Comparison of bond lengths in the bridge with those of known compounds indicates a significant contribution of the canonical form **B** shown in eq 4. The bridging Ta–C distances of 1.96 (2) and 1.935 (5) Å that occur in **3b** and **4**, respectively, are substantially shorter than distances found for compounds having tantalum–carbon single bonds (2.25–2.32 Å) and slightly shorter than those having tantalum–carbon double bonds (2.01–2.03 Å).[21-24] The carbonyl C–O bridge bond distances of 1.27 (2) and 1.269 (6) Å for **3b** and **4**, respectively, are significantly longer than those found in terminal carbonyls and are in fact closer to the value of 1.34 (2) Å occurring in the siloxycarbyne complex $[\mathrm{Ta}\{\equiv\mathrm{COSi}(i\text{-}\mathrm{Pr})_3\}(\mathrm{CO})(\mathrm{dmpe})_2]$.[4]

Spectroscopic Properties of 3a and 4. The bridging Ta=C=O—Ta unit in **3a** has an unusually low stretching frequency of 1462 cm^{-1}, which was identified by a ^{13}C labeling experiment. This low value is a further manifestation of the significant oxycarbyne character of this complex, as discussed above. The observed value is nearly identical to that of 1466 cm^{-1} reported for the carbyne ligand in $[\mathrm{M}\{\equiv\mathrm{COSi}(i\text{-}\mathrm{Pr})_3\}(\mathrm{CO})(\mathrm{dmpe})_2]$ (M = Ta or Nb).[4] The NMR spectra (^{31}P{^{1}H}, ^{1}H, and ^{13}C{^{1}H}) of **3a** and **4** are all consistent with the geometry observed in the solid state for these complexes being maintained in solution.

Conclusions

Two novel carbonyl-bridged dinuclear compounds have been synthesized and structurally characterized. The first of these complexes, **3a**, is formed by the formal disproportionation of two siloxycarbynes in the presence of sodium chloride. Although **3a** reacts with $\mathrm{Me_3SiCl}$ to afford a reductively coupled product, previous work in our laboratory has shown that bridged species of this kind are not likely to be intermediates in the reaction.[5] The heterodimetallic carbonyl-bridged complex **4** has been synthesized by reaction of $\mathrm{Na[Ta(CO)_2(dmpe)_2]}$ with $\mathrm{Cp^*_2ZrCl_2}$. This compound reacts with 2 equiv of $\mathrm{Me_3SiCl}$ to yield the reductively coupled product $\mathrm{[Ta(Me_3SiOCCOSiMe_3)(dmpe)_2Cl]}$.

Acknowledgment. This work was supported by a grant from the National Science Foundation. We thank Drs. J. D. Protasiewicz and S. Yu for helpful comments on the manuscript.

Registry No. **1**, 61916-36-7; **3a**, 137364-76-2; **3b**, 137364-77-3; **4**, 137364-78-4; **5**, 61916-37-8; $\mathrm{Me_3SiCl}$, 75-77-4; $t\text{-}\mathrm{BuMe_2SiCl}$, 18162-48-6; $\mathrm{[Ta(Me_3SiOCCOSiMe_3)(dmpe)_2I]}$, 109467-50-7; $\mathrm{[Ta(Me_3SiOCCOSiMe_3)(dmpe)_2Cl]}$, 99797-93-0; $\mathrm{Cp^*_2ZrCl_2}$, 54039-38-2.

Supplementary Material Available: Tables S1–S6 reporting non-hydrogen atom thermal parameters and hydrogen atom positional and thermal parameters for $[(\mathrm{dmpe})_2(\mathrm{CO})\mathrm{TaCOTa}(t\text{-}\mathrm{BuMe_2SiOCCOSiMe_2}\text{-}t\text{-}\mathrm{Bu})(\mathrm{dmpe})_2]$ and $[(\mathrm{dmpe})_2(\mathrm{CO})\mathrm{TaCOZrCp^*_2Cl}]$ (9 pages); listings of observed and calculated structure factors for $[(\mathrm{dmpe})_2(\mathrm{CO})\mathrm{TaCOTa}(t\text{-}\mathrm{BuMe_2SiOCCOSiMe_2}\text{-}t\text{-}\mathrm{Bu})(\mathrm{dmpe})_2]$ and $[(\mathrm{dmpe})_2(\mathrm{CO})\mathrm{TaCOZrCp^*_2Cl}]$ (65 pages). Ordering information is given on any current masthead page.

---

[21] Gibson, V. C.; Grebenik, P. D.; Green, M. L. H. *J. Chem. Soc., Chem. Commun.* **1983**, 1101.

[22] Guggenberger, L. J.; Schrock, R. R. *J. Am. Chem. Soc.* **1975**, *97*, 6578.

[23] Schrock, R. R.; Messerle, L. W.; Wood, C. D.; Guggenberger, L. J. *J. Am. Chem. Soc.* **1978**, *100*, 3793.

[24] Green, M. L. H.; Hare, P. M.; Bandy, J. A. *J. Organomet. Chem.* **1987**, *330*, 61.

[25] Schneider, M.; Weiss, E. *J. Organomet. Chem.* **1976**, *121*, 365.

[26] Longato, B.; Martin, B. D.; Norton, J. R.; Anderson, O. P. *Inorg. Chem.* **1985**, *24*, 1389.

[27] Tilley, T. D.; Andersen, R. A. *J. Chem. Soc., Chem. Commun.* **1981**, 985.

[28] Boncella, J. M.; Andersen, R. A. *Inorg. Chem.* **1984**, *23*, 432.

[29] Hamilton, D. M., Jr.; Willis, W. S.; Stucky, G. D. *J. Am. Chem. Soc.* **1991**, *103*, 4255.

[30] Tilley, T. D.; Andersen, R. A. *J. Am. Chem. Soc.* **1982**, *104*, 1772.

[31] Marsella, J. A.; Huffman, J. C.; Caulton, K. G.; Longato, B.; Norton, J. R. *J. Am. Chem. Soc.* **1982**, *104*, 6360.

Iron–Osmium Bonding in Clusters Containing Ferrocene Fragments

William R. Cullen,* Steven J. Rettig, and Tu-Cai Zheng

Department of Chemistry, University of British Columbia, Vancouver, British Columbia, Canada V6T 1Z1

Received August 13, 1991

Pyrolysis of $\mathrm{Os_3(CO)_{10}(PFcPh_2)_2}$ and $\mathrm{Os_3(CO)_{11}(PFc_2Ph)}$ affords $\mathrm{Os_3(CO)_8(H)_2[PAr(C_6H_5)(\eta\text{-}C_5H_3)Fe(\eta\text{-}C_5H_4)]}$ (Ar = $\mathrm{C_6H_5}$ (**3a**), Fc (**3b**), respectively). $\mathrm{Os_3(CO)_7(H)(PPr^i)[Fe(\eta\text{-}C_5H_4PPr^i_2)(\eta\text{-}C_5H_4)]}$ (**4**) is a product of the thermolysis of $\mathrm{Os_3(CO)_{10}[Fe(\eta\text{-}C_5H_4PPr^i_2)_2]}$. **3b**: triclinic, space group $P\bar{1}$ (No. 2), $a = 13.878$ (2) Å, $b = 14.145$ (3) Å, $c = 10.698$ (2) Å, $\alpha = 104.28$ (1)°, $\beta = 110.88$ (1)°, $\gamma = 63.91$ (1)°. **3a**: monoclinic, space group $P2_1/c$ (No. 14), $a = 9.484$ (3) Å, $b = 18.144$ (4) Å, $c = 17.421$ (3) Å, $\beta = 90.10$ (2)°. **4**: monoclinic, space group $P2_1/n$ (No. 14), $a = 8.910$ (3) Å, $b = 22.784$ (2) Å, $c = 15.416$ (2) Å, $\beta = 98.25$ (2)°. The complexes are electron precise if the Fe→Os bonds of length 2.830 (1) (**3a**), 2.826 (1) (**3b**), and 2.813 (1) Å (**4**) are included.

There are only a few examples known where the central metal of a metallocene acts as an electron donor to a metal, and most examples are complexes of ferrocene derivatives with the group-8 metals Ni, Pt, and Pd,[1] e.g., complex 1

0276-7333/92/2311-0277$03.00/0 © 1992 American Chemical Society

Table I. Crystallographic Data[a]

compd	**3a**	**3b**·0.5CH$_2$Cl$_2$	**4**
formula	$C_{30}H_{19}FeO_8Os_3P$	$C_{34.5}H_{24}ClFe_2O_8Os_3P$	$C_{26}H_{30}FeO_7Os_3P_2$
fw	1164.90	1315.29	1142.91
cryst syst	monoclinic	triclinic	monoclinic
space group	$P2_1/c$	$P\bar{1}$	$P2_1/n$
a, Å	9.484 (3)	13.878 (2)	8.910 (3)
b, Å	18.144 (4)	14.145 (3)	22.784 (2)
c, Å	17.421 (3)	10.698 (2)	15.416 (2)
α, deg	90	104.28 (1)	90
β, deg	90.10 (2)	101.88 (1)	98.25 (2)
γ, deg	90	63.91 (1)	90
V, Å^3	2998 (2)	1816.4 (5)	3097 (1)
Z	4	2	4
ρ_{calc}, g/cm^3	2.581	2.405	2.451
$F(000)$	2128	1214	2104
μ(Mo Kα), cm^{-1}	132.6	114.2	128.8
transm factors	0.39–1.00	0.79–1.00	0.78–1.00
cryst size, mm	0.22 × 0.30 × 0.43	0.08 × 0.12 × 0.28	0.05 × 0.05 × 0.28
scan type	ω–2θ	ω–2θ	ω–2θ
scan range, deg in ω	1.05 + 0.35 tan θ	1.10 + 0.35 tan θ	0.94 + 0.35 tan θ
scan rate, deg/min	32	32	16
data collcd	$+h,+k,\pm l$	$+h,\pm k,\pm l$	$+h,+k,\pm l$
$2\theta_{max}$, deg	60	60	60
cryst decay	negligible	6.1%	negligible
total no. of reflns	9497	10981	9818
no. of unique rflns	9051	10570	9278
R_{merge}	0.064	0.037	0.064
rflns with $I > 3\sigma(I)$	5193	6374	4114
no. of variables	389	445	352
R	0.038	0.027	0.032
R_w	0.042	0.028	0.026
gof	1.55	1.27	1.16
max Δ/σ (final cycle)	0.01	0.16	0.04
residual density, e/Å^3	−1.8 to +1.8 (near Os)	−1.0 to +0.8	−0.9 to +0.9

[a] Temperature 294 K, Rigaku AFC6S diffractometer, Mo Kα radiation (λ = 0.71069 Å), graphite monochromator, takeoff angle 6.0°, aperture 6.0 × 6.0 mm at a distance of 285 mm from the crystal, stationary background counts at each end of the scan (scan/background time ratio 2:1, up to eight rescans), $\sigma^2(F^2) = [S^2(C + 4B) + (pF^2)^2]/Lp^2$ (S = scan rate, C = scan count, B = normalized background count, p = 0.025 for **3a**, 0.02 for **3b**, and 0.01 for **4**), function minimized $\sum w(|F_0| - |F_c|)^2$ where $w = 4F_0^2/\sigma^2(F_0^2)$, $R = \sum||F_0| - |F_c||/\sum|F_0|$, $R_w = (\sum w(|F_0| - |F_c|)^2/\sum w|F_0|^2)^{1/2}$, and gof $= [\sum \omega(|F_0| - |F_c|)^2/(m - n)]^{1/2}$. Values given for R, R_w, and gof are based on those reflections with $I \geq 3\sigma(I)$.

where the Fe→Pt bond has a length of 2.935 (2) Å. Compound **2**, which is a product of the thermal decomposition of $Ru_3(CO)_{10}[Fe(\eta\text{-}C_5H_4PPh_2)_2]$, is the first example of such bonding in a metal cluster (Fe→Ru = 3.098 (3) Å).[2] One of the C$_5$ rings in **2** is also metalated. We now report the structures of three osmium cluster derivatives, $Os_3(CO)_8(H)_2PAr(C_6H_5)(\eta\text{-}C_5H_3)Fe(\eta\text{-}C_5H_4)$(Ar = C$_6H_5$ (**3a**), Fc (**3b**)) and $Os_3(CO)_7(H)(\mu_3\text{-}PPr^i)[Fe(\eta\text{-}C_5H_4PPr^i{}_2)(\eta\text{-}C_5H_4)]$ (**4**), that show strong iron–osmium interactions. *Both* C$_5$-rings of the ferrocene moiety are activated in the formation of **3** by metalation reactions. Phosphorus–carbon bond cleavage, both P–C(sp^2) and P–C(sp^3), accompanies the formation of **4**.

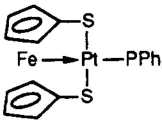

1

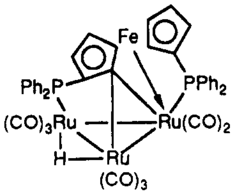

2

Experimental Section

The experimental procedures and instrumentation used in this work have been described previously.[3]

Preparation of $Os_3(CO)_8(H)_2PPh_2(\eta\text{-}C_5H_3)Fe(\eta\text{-}C_5H_4)$ (3a). A solution of $Os_3(CO)_{10}(PFcPh_2)_2$ (150 mg, 0.094 mmol) in octane (50 mL) was refluxed under an Ar atmosphere until no more starting material was present (5 h, TLC monitoring). The solvent was removed in vacuo and the residue was chromatographed on silica with 3:1 petroleum ether/CH$_2$Cl$_2$ as eluent. The third band proved to be **3a** (15% yield), and suitable crystals for X-ray studies were obtained by slow evaporation of the isolated fraction. $^{31}P\{^1H\}$ NMR (200 MHz, CDCl$_3$): δ −6.0 ppm. ^{1}H NMR (200 MHz, CDCl$_3$): δ −16.95 (d, J = 13.4 Hz, 1 H), −12.25 (d, J = 4.6 Hz, 1 H), 2.9 (m, 1 H), 3.1 (m, 1 H), 4.0 (m, 1 H), 4.2 (m, 1 H), 4.6 (m, 1 H), 5.2 (m, 2 H), 7.20–7.35 (bm, 10 H). FAB mass spectrum: m/e 1164 (P$^+$) with successive loss of 8 CO's and 1 Ph. Anal. Calcd for $C_{30}H_{19}FeO_8Os_3P$: C, 30.93: H, 1.64. Found: C, 31.20: H, 1.71.

Preparation of $Os_3(CO)_8(H)_2PPh(\eta\text{-}C_5H_4)Fe(\eta\text{-}C_5H_5)(\eta\text{-}C_5H_3)Fe(\eta\text{-}C_5H_4)$ (3b). A solution of $Os_3(CO)_{11}PFc_2Ph$ (100 mg, 0.074 mmol) in octane (80 mL) was heated to reflux for 3 h. Six compounds were produced in moderate yield, as judged by TLC, and they were separated by column chromatography by using 4:1 petroleum ether/CH$_2$Cl$_2$ as eluent. The third band, which contained **3b** (15% yield), was collected: the solute was isolated and recrystallized from a 1:1 mixture of petroleum ether/CH$_2$Cl$_2$. ^{1}H NMR (500 MHz, CDCl$_3$): δ −16.91 (d, J = 12.5 Hz, 1 H), −12.13 (d, J = 4.5 Hz, 1 H), 3.08 (m, 1 H), 3.36 (m, 1 H), 3.42 (m, 1 H), 4.02 (s, 5 H), 4.08 (m, 1 H), 4.30–4.45 (m, 3 H), 4.55 (m, 1 H), 4.64

---

(1) (a) Seyferth, D.; Hames, B. W.; Rucker, T. G.; Cowie, M.; Dickson, R. S. *Organometallics* **1983**, *2*, 472. (b) Sato, M.; Sekino, M.; Akabori, S. *J. Organomet. Chem.* **1988**, *C31*, 344. (c) Sato, M.; Suzuki, K.; Akabori, S. *Chem. Lett.* **1987**, 2239. (d) Akabori, S.; Kumagai, T.; Shirahige, T.; Sato, S.; Kawazoe, K.; Tamura, C.; Sato, M. *Organometallics* **1987**, *6*, 526.

(2) Bruce, M. I.; Humphrey, P. A.; Shawkataly, O. B.; Snow, M. R.; Tiekink, E. R. T.; Cullen, W. R. *Organometallics* **1990**, *9*, 2910.

(3) Cullen, W. R.; Chacon, S. T.; Bruce, M. I.; Einstein, F. W. B.; Jones, R. H. *Organometallics* **1988**, *7*, 2273.

Table II. Final Atomic Coordinates (Fractional) and B_{eq} Values (Å^2)[a] for 3b

atom	x	y	z	B_{eq}
Os(1)	0.12572 (2)	0.21063 (2)	0.20583 (2)	3.22 (1)
Os(2)	0.23187 (2)	0.36509 (2)	0.35898 (2)	2.79 (1)
Os(3)	0.33424 (2)	0.13646 (2)	0.34886 (2)	2.91 (1)
Fe(1)	0.21489 (6)	0.17852 (7)	−0.02427 (8)	3.20 (5)
Fe(2)	0.28778 (7)	0.56129 (8)	0.0595 (1)	3.97 (5)
P(1)	0.3341 (1)	0.3296 (1)	0.1837 (1)	2.61 (7)
O(1)	0.0879 (6)	0.0103 (6)	0.1324 (7)	8.4 (6)
O(2)	−0.0736 (4)	0.3227 (6)	0.3426 (6)	7.1 (4)
O(3)	0.4178 (4)	0.3596 (5)	0.5677 (5)	5.9 (4)
O(4)	0.1231 (5)	0.6053 (4)	0.3615 (5)	6.2 (4)
O(5)	0.0998 (4)	0.3898 (5)	0.5703 (5)	6.2 (4)
O(6)	0.5686 (4)	0.1066 (4)	0.3943 (5)	5.4 (3)
O(7)	0.3989 (5)	−0.1039 (5)	0.2935 (6)	7.6 (4)
O(8)	0.3279 (5)	0.1666 (5)	0.6401 (4)	6.5 (4)
C(1)	0.1014 (7)	0.0873 (7)	0.1579 (7)	5.5 (6)
C(2)	0.0064 (5)	0.2780 (6)	0.2948 (7)	4.6 (4)
C(3)	0.3489 (5)	0.3622 (5)	0.4864 (6)	3.8 (4)
C(4)	0.1628 (5)	0.5145 (6)	0.3578 (6)	4.0 (4)
C(5)	0.1489 (5)	0.3773 (6)	0.4901 (6)	4.0 (4)
C(6)	0.4801 (5)	0.1199 (5)	0.3738 (6)	3.6 (4)
C(7)	0.3751 (6)	−0.0135 (6)	0.3170 (7)	4.8 (5)
C(8)	0.3311 (5)	0.1564 (6)	0.5310 (6)	4.0 (4)
C(9)	0.3229 (4)	0.1296 (5)	0.1438 (5)	2.9 (3)
C(10)	0.3413 (4)	0.2040 (5)	0.0877 (5)	2.8 (3)
C(11)	0.3647 (4)	0.1594 (5)	−0.0443 (5)	3.2 (3)
C(12)	0.3591 (5)	0.0598 (5)	−0.0748 (6)	3.6 (3)
C(13)	0.3328 (5)	0.0425 (5)	0.0360 (6)	3.5 (3)
C(14)	0.0661 (5)	0.2425 (6)	0.0203 (6)	3.8 (4)
C(15)	0.0823 (5)	0.3214 (6)	−0.0234 (6)	3.8 (4)
C(16)	0.1118 (5)	0.2812 (7)	−0.1509 (6)	4.8 (5)
C(17)	0.1089 (6)	0.1782 (7)	−0.1936 (6)	5.2 (5)
C(18)	0.0771 (5)	0.1568 (6)	−0.0906 (7)	4.7 (4)
C(19)	0.2879 (4)	0.4181 (5)	0.0680 (5)	3.0 (3)
C(20)	0.1804 (5)	0.4958 (5)	0.0383 (6)	3.6 (3)
C(21)	0.1763 (5)	0.5270 (6)	−0.0780 (7)	4.6 (4)
C(22)	0.2798 (6)	0.4729 (6)	−0.1208 (7)	5.0 (5)
C(23)	0.3490 (5)	0.4060 (5)	−0.0325 (6)	4.0 (4)
C(24)	0.3246 (7)	0.6424 (7)	0.2368 (8)	5.8 (6)
C(25)	0.2273 (7)	0.7093 (7)	0.175 (1)	6.4 (6)
C(26)	0.2500 (8)	0.7171 (7)	0.058 (1)	6.8 (6)
C(27)	0.3603 (7)	0.6550 (7)	0.046 (1)	6.4 (6)
C(28)	0.4059 (7)	0.6097 (7)	0.1571 (9)	5.8 (5)
C(29)	0.4754 (4)	0.3108 (5)	0.2286 (5)	2.8 (3)
C(30)	0.5582 (5)	0.2214 (5)	0.1705 (6)	3.5 (3)
C(31)	0.6652 (5)	0.2089 (6)	0.2077 (7)	4.5 (4)
C(32)	0.6888 (5)	0.2834 (7)	0.2983 (8)	4.9 (5)
C(33)	0.6070 (6)	0.3726 (7)	0.3537 (7)	5.0 (5)
C(34)	0.5017 (5)	0.3857 (5)	0.3204 (6)	4.0 (4)
Cl(1)[b]	−0.006 (5)	0.070 (4)	0.468 (4)	35 (2)
Cl(1A)[b]	−0.073 (3)	0.057 (4)	0.527 (3)	29 (1)
Cl(2)	−0.170 (2)	0.058 (2)	0.525 (2)	27.6 (8)
H(1)	0.1633	0.3102	0.2447	3.9
H(2)	0.1971	0.1720	0.3478	3.9

[a] $B_{eq} = (8/3)\ \pi^2 \sum\sum U_{ij} a_i^* a_j^* (a_i \cdot a_j)$. [b] Atoms Cl(1) and Cl(1A) were refined as 50% Cl and 50% C; see Experimental section.

Table III. Bond Lengths (Å) with Estimated Standard Deviations[a] for 3b

Os(1)–Os(3)	2.8488 (6)	Fe(2)–Cp(3)	1.641 (3)
Os(1)–Fe(1)	2.830 (1)	Fe(2)–Cp(4)	1.661 (5)
Os(1)–C(1)	1.851 (9)	P(1)–C(10)	1.791 (6)
Os(1)–C(2)	1.836 (7)	P(1)–C(19)	1.801 (6)
Os(1)–C(14)	2.065 (6)	P(1)–C(29)	1.833 (5)
Os(1)–H(1)	1.64	O(1)–C(1)	1.143 (9)
Os(1)–H(2)	1.70	O(2)–C(2)	1.162 (8)
Os(2)–Os(3)	2.8876 (7)	O(3)–C(3)	1.147 (7)
Os(2)–P(1)	2.405 (1)	O(4)–C(4)	1.147 (8)
Os(2)–C(3)	1.886 (7)	O(5)–C(5)	1.137 (7)
Os(2)–C(4)	1.901 (7)	O(6)–C(6)	1.140 (7)
Os(2)–C(5)	1.922 (6)	O(7)–C(7)	1.144 (9)
Os(2)–H(1)	1.64	O(8)–C(8)	1.148 (7)
Os(3)–C(6)	1.901 (7)	C(9)–C(10)	1.465 (8)
Os(3)–C(7)	1.898 (8)	C(9)–C(13)	1.443 (8)
Os(3)–C(8)	1.905 (6)	C(10)–C(11)	1.437 (7)
Os(3)–C(9)	2.148 (6)	C(11)–C(12)	1.398 (9)
Os(3)–H(2)	1.74	C(12)–C(13)	1.414 (8)
Fe(1)–C(9)	2.134 (5)	C(14)–C(15)	1.43 (1)
Fe(1)–C(10)	2.030 (6)	C(14)–C(18)	1.45 (1)
Fe(1)–C(11)	2.026 (6)	C(15)–C(16)	1.412 (9)
Fe(1)–C(12)	2.039 (6)	C(16)–C(17)	1.41 (1)
Fe(1)–C(13)	2.051 (6)	C(17)–C(18)	1.41 (1)
Fe(1)–C(14)	1.964 (6)	C(19)–C(20)	1.439 (8)
Fe(1)–C(15)	2.048 (6)	C(19)–C(23)	1.436 (8)
Fe(1)–C(16)	2.082 (7)	C(20)–C(21)	1.402 (9)
Fe(1)–C(17)	2.086 (7)	C(21)–C(22)	1.411 (9)
Fe(1)–C(18)	2.027 (7)	C(22)–C(23)	1.406 (9)
Fe(1)–Cp(1)	1.657 (3)	C(24)–C(25)	1.40 (1)
Fe(1)–Cp(2)	1.643 (4)	C(24)–C(28)	1.40 (1)
Fe(2)–C(19)	2.049 (6)	C(25)–C(26)	1.39 (1)
Fe(2)–C(20)	2.025 (7)	C(26)–C(27)	1.41 (1)
Fe(2)–C(21)	2.040 (7)	C(27)–C(28)	1.39 (1)
Fe(2)–C(22)	2.035 (8)	C(29)–C(30)	1.390 (8)
Fe(2)–C(23)	2.038 (7)	C(29)–C(34)	1.379 (8)
Fe(2)–C(24)	2.054 (9)	C(30)–C(31)	1.398 (9)
Fe(2)–C(25)	2.056 (8)	C(31)–C(32)	1.35 (1)
Fe(2)–C(26)	2.032 (8)	C(32)–C(33)	1.37 (1)
Fe(2)–C(27)	2.032 (8)	C(33)–C(34)	1.37 (1)
Fe(2)–C(28)	2.044 (8)		

[a] Here and elsewhere, Cp(1–4) refers to the centroids of the cyclopentadienyl ring.

(m, 1 H), 5.00–5.10 (m, 2 H), 7.34–7.50 (bm, 3 H), 7.60–7.76 (bm, 2 H). $^{31}P\{^1H\}$ NMR (121.4 MHz, $CDCL_3$): δ −20.4. FAB mass spectrum: m/e 1274 (P^+) with successive loss of 8 CO's. Anal. Calcd for $C_{34}H_{23}Fe_2O_8Os_3P{\cdot}0.5CH_2Cl_2$: C, 31.50; H, 1.84. Found: C, 32.60; H, 1.85.

Preparation of $Os_3(CO)_7(H)(PPr^i)[Fe(\eta\text{-}C_5H_4PPr^i{}_2)(\eta\text{-}C_5H_4)$ (4). A solution of $Os_3(CO)_{10}[Fe(\eta\text{-}C_5H_4PPr^i{}_2)]$ (100 mg, 0.079 mmol) in octane (50 mL) was refluxed for 7.5 h. Evaporation of the solvent followed by chromatography on silica by using 3:1 petroleum ether/CH_2Cl_2 as eluent yielded a number of bands. The sixth band afforded 4 after evaporation of the solvent in 15% yield. $^{31}P\{^1H\}$ NMR (121.4 MHz, $CDCl_3$): δ 268.3, 16.5. ^1H NMR (400 MHz, $CDCl_3$): δ −21.9 (dd, J_1 = 17.5 Hz, J_2 = 7.6 Hz, 1 H), 1.39 (dd, 3 H), 1.47 (dd, 3 H), 1.51 (dd, 3 H), 1.57 (dd, 3 H), 1.84 (dd, 3 H), 1.88 (dd, 3 H), 2.08 (d of septets, 1 H), 2.56 (d of septets, 1 H), 2.87 (bm, 1 H), 3.22 (bm, 1 H), 3.51 (bm, 1 H), 3.65 (d of septets, 1 H), 3.82 (bm, 1 H), 4.86 (bm, 1 H), 4.89 (bm, 1 H), 5.17 (bm, 1 H), 5.21 (bm, 1 H). FAB mass spectrum: m/e 1142 (P^+) and fragments associated with loss of 7 CO and 3 Pr^i groups.

X-ray Analysis of 3b. All measurements were made on a Rigaku AFC6S diffractometer with graphite-monochromated Mo Kα radiation. Crystal data appear in Table I. The final unit-cell parameters were obtained by least squares on the setting angles for 25 reflections with 2θ = 32.33–36.80°. The intensities of three representative reflections which were measured every 200 reflections declined by 6.10%. A linear correction factor was applied to the data to account for this phenomenon. The data were processed[4] and corrected for Lorentz and polarization effects and absorption.

The structure was solved by a combination of the Patterson method and direct methods. The non-hydrogen atoms were refined either anisotropically or isotropically (for the disordered

---

(4) (a) Cromer, D. T.; Waber, J. T. *International Tables for X-Ray Crystallography*; The Kynoch Press: Birmingham, England, 1974; Vol. IV, Table 2.2 A. (b) Ibers, J. A.; Hamilton, W. C. *Acta Crystallogr.* 1964, *17*, 781. (c) Cromer, D. T. *International Tables for X-Ray Crystallography*; The Kynoch Press; Birmingham, England, 1974; Vol. IV, Table 2.3.1. (d) *TEXSAN-TEXRAY Structure Analysis Package*; Molecular Structure Corp.: Woodlands, TX, 1985. (e) Motherwell, S.; Clegg, W. *PLUTO program for plotting molecular and crystal structures*; University of Cambridge: Cambridge, England, 1978. (f) Johnson, C. K. ORTEPII; Report ORNL-5138; Oak Ridge National Laboratory; Oak Ridge, TN, 1976. (g) Calbrese, J. C. PHASE: Patterson Heavy Atom Solution Extractor. Ph.D. Thesis, University of Wisconsin-Madison, 1972. (h) Beurskens, P. T. DIRDIF: *Direct Methods for Difference Structures—an automatic procedure for phase extension and refinement of difference structure factors*; Technical Report 1984/I; Crystallography Laboratory: Toevnooiveld, 6525 Ed Nijmegan, Netherlands, 1984.

Table IV. Bond Angles (deg) with Estimated Standard Deviations for 3b

Os(3)–Os(1)–Fe(1)	91.76 (2)	C(9)–Os(3)–H(2)	94
Os(3)–Os(1)–C(1)	101.6 (2)	Os(1)–Fe(1)–Cp(1)	98.4 (1)
Os(3)–Os(1)–C(2)	118.8 (2)	Os(1)–Fe(1)–Cp(2)	85.6 (1)
Os(3)–Os(1)–C(14)	135.4 (2)	Cp(1)–Fe(1)–Cp(2)	176.1 (2)
Os(3)–Os(1)–H(1)	73	Cp(3)–Fe(2)–Cp(4)	174.6 (2)
Os(3)–Os(1)–H(2)	35	Os(2)–P(1)–C(10)	106.4 (2)
Fe(1)–Os(1)–C(1)	94.4 (3)	Os(2)–P(1)–C(19)	121.2 (2)
Fe(1)–Os(1)–C(2)	147.3 (2)	Os(2)–P(1)–C(29)	116.5 (2)
Fe(1)–Os(1)–C(14)	44.0 (2)	C(10)–P(1)–C(19)	104.3 (3)
Fe(1)–Os(1)–H(1)	81	C(10)–P(1)–C(29)	104.5 (3)
Fe(1)–Os(1)–H(2)	126	C(19)–P(1)–C(29)	102.2 (3)
C(1)–Os(1)–C(2)	90.7 (4)	Os(1)–C(1)–O(1)	177.7 (7)
C(1)–Os(1)–C(14)	89.2 (3)	Os(1)–C(2)–O(2)	175.0 (6)
C(1)–Os(1)–H(1)	173	Os(2)–C(3)–O(3)	176.8 (6)
C(1)–Os(1)–H(2)	91	Os(2)–C(4)–O(4)	177.5 (7)
C(2)–Os(1)–C(14)	104.0 (3)	Os(2)–C(5)–O(5)	176.3 (7)
C(2)–Os(1)–H(1)	96	Os(3)–C(6)–O(6)	176.0 (6)
C(2)–Os(1)–H(2)	86	Os(3)–C(7)–O(7)	177.7 (7)
C(14)–Os(1)–H(1)	92	Os(3)–C(8)–O(8)	178.2 (7)
C(14)–Os(1)–H(2)	170	Os(3)–C(9)–C(10)	123.6 (4)
H(1)–Os(1)–H(2)	87	Os(3)–C(9)–C(13)	131.1 (4)
Os(3)–Os(2)–P(1)	85.20 (4)	C(10)–C(9)–C(13)	102.3 (5)
Os(3)–Os(2)–C(3)	82.8 (2)	P(1)–C(10)–C(9)	120.0 (4)
Os(3)–Os(2)–C(4)	177.5 (2)	P(1)–C(10)–C(11)	129.7 (5)
Os(3)–Os(2)–C(5)	89.1 (2)	C(9)–C(10)–C(11)	110.4 (5)
Os(3)–Os(2)–H(1)	72	C(10)–C(11)–C(12)	107.5 (5)
P(1)–Os(2)–C(3)	93.0 (2)	C(11)–C(12)–C(13)	107.9 (5)
P(1)–Os(2)–C(4)	93.2 (2)	C(9)–C(13)–C(12)	111.9 (6)
P(1)–Os(2)–C(5)	173.1 (2)	Os(1)–C(14)–C(15)	120.5 (5)
P(1)–Os(2)–H(1)	82	Os(1)–C(14)–C(18)	121.2 (5)
C(3)–Os(2)–C(4)	99.1 (3)	C(15)–C(14)–C(18)	105.5 (6)
C(3)–Os(2)–C(5)	90.2 (3)	C(14)–C(15)–C(16)	108.9 (7)
C(3)–Os(2)–H(1)	154	C(15)–C(16)–C(17)	109.0 (7)
C(4)–Os(2)–C(5)	92.4 (3)	C(16)–C(17)–C(18)	106.5 (6)
C(4)–Os(2)–H(1)	106	C(14)–C(18)–C(17)	109.9 (7)
C(5)–Os(2)–H(1)	92	P(1)–C(19)–C(20)	128.3 (4)
Os(1)–Os(3)–Os(2)	65.76 (2)	P(1)–C(19)–C(23)	123.9 (4)
Os(1)–Os(3)–C(6)	149.0 (2)	C(20)–C(19)–C(23)	106.5 (5)
Os(1)–Os(3)–C(7)	102.0 (2)	C(19)–C(20)–C(21)	108.3 (5)
Os(1)–Os(3)–C(8)	113.8 (2)	C(20)–C(21)–C(22)	108.4 (5)
Os(1)–Os(3)–C(9)	61.3 (1)	C(21)–C(22)–C(23)	108.6 (6)
Os(1)–Os(3)–H(2)	34	C(19)–C(23)–C(22)	108.1 (5)
Os(2)–Os(3)–C(6)	97.9 (2)	C(25)–C(24)–C(28)	108.3 (8)
Os(2)–Os(3)–C(7)	167.7 (2)	C(24)–C(25)–C(26)	107.1 (8)
Os(2)–Os(3)–C(8)	90.4 (2)	C(25)–C(26)–C(27)	109.2 (8)
Os(2)–Os(3)–C(9)	84.2 (2)	C(26)–C(27)–C(28)	107.0 (8)
Os(2)–Os(3)–H(2)	75	C(24)–C(28)–C(27)	108.5 (7)
C(6)–Os(3)–C(7)	92.6 (3)	P(1)–C(29)–C(30)	121.0 (5)
C(6)–Os(3)–C(8)	91.5 (3)	P(1)–C(29)–C(34)	120.5 (4)
C(6)–Os(3)–C(9)	92.1 (2)	C(30)–C(29)–C(34)	118.5 (5)
C(6)–Os(3)–H(2)	170	C(29)–C(30)–C(31)	119.7 (6)
C(7)–Os(3)–C(8)	95.8 (3)	C(30)–C(31)–C(32)	120.7 (6)
C(7)–Os(3)–C(9)	88.9 (3)	C(31)–C(32)–C(33)	119.7 (6)
C(7)–Os(3)–H(2)	96	C(32)–C(33)–C(34)	120.7 (7)
C(8)–Os(3)–C(9)	173.9 (2)	C(29)–C(34)–C(33)	120.8 (6)
C(8)–Os(3)–H(2)	82		

CH_2Cl_2 solvate). The metal hydride atoms were included in difference map positions but were not refined. All other hydrogen atoms were fixed in calculated positions with C–H = 0.98 Å. Neutral-atom scattering factors and anomalous dispersion corrections for the non-hydrogen atom were taken from ref 4a,c. Final atomic coordinates and equivalent isotropic thermal parameters, bond lengths, and bond angles appear in Tables II–X.

X-ray Analysis of 3a and 4. The data collection, structure solution, and refinement proceeded as for **3b**. Relevant data are given in Table I. Final atomic coordinates and equivalent isotropic thermal parameters, bond lengths, and bond angles appear in Tables II–X.

Table V. Final Atomic Coordinates (Fractional) and B_{eq} Values ($Å^2$)[a] for 3a

atom	x	y	z	B_{eq}
Os(1)	0.24441 (4)	0.16890 (2)	0.07774 (2)	2.38 (2)
Os(2)	0.14274 (4)	0.03650 (2)	0.17212 (2)	2.29 (1)
Os(3)	0.43595 (4)	0.07424 (2)	0.15580 (2)	2.44 (2)
Fe(1)	0.2353 (1)	0.26693 (8)	0.20369 (8)	2.65 (6)
P(1)	0.1520 (2)	0.1070 (1)	0.2889 (1)	2.3 (1)
O(1)	0.4579 (9)	0.2584 (5)	−0.0082 (5)	5.1 (4)
O(2)	0.111 (1)	0.1243 (5)	−0.0699 (4)	5.1 (4)
O(3)	0.268 (1)	−0.0998 (5)	0.2481 (5)	5.1 (4)
O(4)	−0.1682 (8)	−0.0038 (5)	0.1819 (5)	4.7 (4)
O(5)	0.166 (1)	−0.0372 (5)	0.0140 (5)	5.2 (4)
O(6)	0.5542 (9)	0.0133 (5)	0.3053 (5)	5.1 (4)
O(7)	0.7091 (9)	0.1474 (5)	0.1068 (5)	5.3 (5)
O(8)	0.498 (1)	−0.0737 (5)	0.0791 (5)	5.5 (5)
C(1)	0.373 (1)	0.2259 (6)	0.0240 (6)	3.0 (4)
C(2)	0.163 (1)	0.1393 (6)	−0.0132 (6)	3.2 (5)
C(3)	0.221 (1)	−0.0478 (6)	0.2218 (6)	3.3 (5)
C(4)	−0.053 (1)	0.0143 (6)	0.1786 (6)	3.2 (5)
C(5)	0.159 (1)	−0.0085 (6)	0.0734 (5)	3.1 (4)
C(6)	0.507 (1)	0.0378 (7)	0.2513 (6)	3.7 (5)
C(7)	0.609 (1)	0.1191 (7)	0.1249 (6)	3.6 (5)
C(8)	0.474 (1)	−0.0190 (6)	0.1065 (6)	4.0 (5)
C(9)	0.373 (1)	0.1769 (5)	0.2082 (5)	3.0 (4)
C(10)	0.275 (1)	0.1811 (5)	0.2734 (5)	2.4 (4)
C(11)	0.294 (1)	0.2485 (6)	0.3134 (5)	2.9 (4)
C(12)	0.401 (1)	0.2896 (6)	0.2754 (6)	3.6 (5)
C(13)	0.448 (1)	0.2466 (6)	0.2129 (6)	3.1 (4)
C(14)	0.131 (1)	0.2620 (6)	0.1063 (5)	2.7 (4)
C(15)	0.032 (1)	0.2628 (6)	0.1674 (6)	3.2 (5)
C(16)	0.050 (1)	0.3272 (7)	0.2102 (7)	4.4 (6)
C(17)	0.160 (1)	0.3695 (6)	0.1770 (7)	4.6 (6)
C(18)	0.206 (1)	0.3332 (6)	0.1116 (6)	3.9 (5)
C(19)	−0.005(1)	0.1516 (6)	0.3293 (6)	2.9 (4)
C(20)	0.005 (1)	0.1857 (6)	0.4024 (6)	3.4 (5)
C(21)	−0.105 (1)	0.2237 (7)	0.4326 (6)	4.1 (5)
C(22)	−0.230 (1)	0.2246 (8)	0.3930 (8)	5.5 (7)
C(23)	−0.248 (1)	0.1899 (8)	0.3236 (7)	4.6 (6)
C(24)	−0.132 (1)	0.1531 (6)	0.2926 (6)	3.5 (5)
C(25)	0.210 (1)	0.0548 (6)	0.3727 (5)	3.0 (4)
C(26)	0.316 (1)	0.0761 (6)	0.4203 (6)	4.0 (5)
C(27)	0.344 (2)	0.037 (1)	0.4869 (7)	6.3 (8)
C(28)	0.264 (2)	−0.023 (1)	0.5047 (8)	7 (1)
C(29)	0.154 (2)	−0.0436 (9)	0.458 (1)	6.5 (9)
C(30)	0.127 (1)	−0.0056 (7)	0.3916 (7)	4.3 (6)
H(1)	0.1212	0.1075	0.1263	2.8
H(2)	0.3435	0.1052	0.0853	2.8

[a] $B_{eq} = (8/3)\pi^2\sum\sum U_{ij}a_i^*a_j^*(a_i \cdot a_j)$.

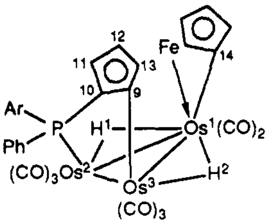

3a: Ar = C_6H_5
3b: Ar = Fe(η-C_5H_5)(η-C_5H_4)

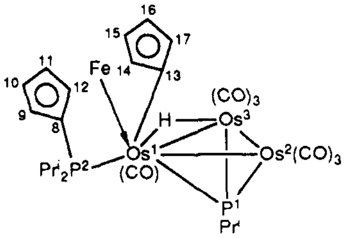

4

Results and Discussion

The complexes **3a** and **3b** are products of the thermal decomposition of $Os_3(CO)_{10}(PFcPh_2)_2$ and $Os_3(CO)_{11}(PFc_2Ph)$, respectively. The formation of **3b** poses no conceptual problems.[2,5] The complex is the result of metalation of the P-substituted C_5 ring accompanied by C–H activation of the second ring and formation of the Fe→Os bond, with all three steps being accompanied by CO loss. This same sequence would account for the formation of **3a** if loss of $PFcPh_2$ accompanied, e.g., the formation of the Fe→Os bond; $Os_3(CO)_{11}(PFcPh_2)$ does not afford **3a** on pyrolysis.

---

(5) The thermal decomposition of $Os_3(CO)_{11}PFc_2Ph$ also affords the novel ferrocyne and benzyne complexes $Os_3(CO)_9$(aryne)PFc.[6]

Table VI. Bond Lengths (Å) with Estimated Standard Deviations[a] for 3a

Os(1)–Os(3)	2.8445 (8)	P(1)–C(25)	1.82 (1)
Os(1)–Fe(1)	2.826 (1)	O(1)–C(1)	1.14 (1)
Os(1)–C(1)	1.86 (1)	O(2)–C(2)	1.14 (1)
Os(1)–C(2)	1.84 (1)	O(3)–C(3)	1.14 (1)
Os(1)–C(14)	2.07 (1)	O(4)–C(4)	1.14 (1)
Os(1)–H(1)	1.82	O(5)–C(5)	1.16 (1)
Os(1)–H(2)	1.50	O(6)–C(6)	1.13 (1)
Os(2)–Os(3)	2.878 (1)	O(7)–C(7)	1.13 (1)
Os(2)–P(1)	2.406 (2)	O(8)–C(8)	1.13 (1)
Os(2)–C(3)	1.91 (1)	C(9)–C(10)	1.47 (1)
Os(2)–C(4)	1.90 (1)	C(9)–C(13)	1.45 (1)
Os(2)–C(5)	1.91 (1)	C(10)–C(11)	1.42 (1)
Os(2)–H(1)	1.53	C(11)–C(12)	1.43 (1)
Os(3)–C(6)	1.91 (1)	C(12)–C(13)	1.41 (1)
Os(3)–C(7)	1.91 (1)	C(14)–C(15)	1.42 (1)
Os(3)–C(8)	1.93 (1)	C(14)–C(18)	1.48 (1)
Os(3)–C(9)	2.16 (1)	C(15)–C(16)	1.40 (2)
Os(3)–H(2)	1.61	C(16)–C(17)	1.42 (2)
Fe(1)–C(9)	2.09 (1)	C(17)–C(18)	1.38 (2)
Fe(1)–C(10)	2.01 (1)	C(19)–C(20)	1.42 (1)
Fe(1)–C(11)	2.02 (1)	C(19)–C(24)	1.37 (1)
Fe(1)–C(12)	2.05 (1)	C(20)–C(21)	1.36 (1)
Fe(1)–C(13)	2.06 (1)	C(21)–C(22)	1.37 (2)
Fe(1)–C(14)	1.97 (1)	C(22)–C(23)	1.37 (2)
Fe(1)–C(15)	2.03 (1)	C(23)–C(24)	1.39 (1)
Fe(1)–C(16)	2.07 (1)	C(25)–C(26)	1.36 (1)
Fe(1)–C(17)	2.05 (1)	C(25)–C(30)	1.39 (2)
Fe(1)–C(18)	2.02 (1)	C(26)–C(27)	1.38 (2)
Fe(1)–Cp(1)	1.640 (5)	C(27)–C(28)	1.36 (2)
Fe(1)–Cp(2)	1.629 (5)	C(28)–C(29)	1.38 (2)
P(1)–C(10)	1.80 (1)	C(29)–C(30)	1.37 (2)
P(1)–C(19)	1.836 (9)		

[a] Here and elsewhere, Cp(1) and Cp(2) refer to the centroids of the C(9–13) and C(14–18) cyclopentadienyl rings, respectively.

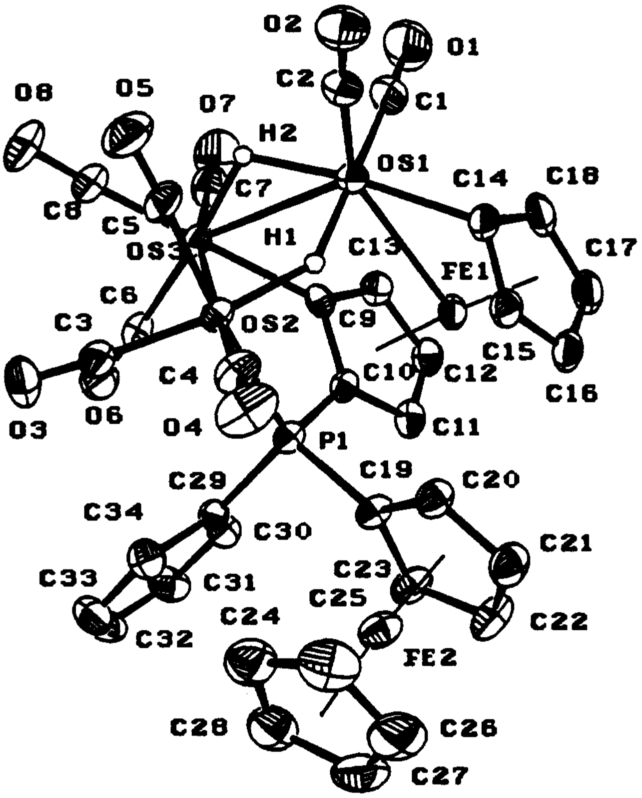

Figure 1. ORTEP plot for 3b.

Table VII. Bond Angles (deg) with Estimated Standard Deviations for 3a

Os(3)–Os(1)–Fe(1)	91.67 (4)	C(8)–Os(3)–C(9)	174.8 (5)
Os(3)–Os(1)–C(1)	99.0 (3)	C(8)–Os(3)–H(2)	94
Os(3)–Os(1)–C(2)	120.1 (3)	C(9)–Os(3)–H(2)	83
Os(3)–Os(1)–C(14)	135.4 (3)	Os(1)–Fe(1)–Cp(1)	98.4 (2)
Os(3)–Os(1)–H(1)	80	Os(1)–Fe(1)–Cp(2)	85.5 (2)
Os(3)–Os(1)–H(2)	25	Cp(1)–Fe(1)–Cp(2)	175.6 (3)
Fe(1)–Os(1)–C(1)	93.6 (3)	Os(2)–P(1)–C(10)	107.0 (3)
Fe(1)–Os(1)–C(2)	147.0 (3)	Os(2)–P(1)–C(19)	122.0 (3)
Fe(1)–Os(1)–C(14)	44.1 (3)	Os(2)–P(1)–C(25)	114.3 (3)
Fe(1)–Os(1)–H(1)	90	C(10)–P(1)–C(19)	104.7 (5)
Fe(1)–Os(1)–H(2)	116	C(10)–P(1)–C(25)	108.4 (5)
C(1)–Os(1)–C(2)	90.3 (4)	C(19)–P(1)–C(25)	99.5 (4)
C(1)–Os(1)–C(14)	90.6 (4)	Os(1)–C(1)–O(1)	177 (1)
C(1)–Os(1)–H(1)	176	Os(1)–C(2)–O(2)	177 (1)
C(1)–Os(1)–H(2)	93	Os(2)–C(3)–O(3)	177 (1)
C(2)–Os(1)–C(14)	103.2 (4)	Os(2)–C(4)–O(4)	176 (1)
C(2)–Os(1)–H(1)	87	Os(2)–C(5)–O(5)	178 (1)
C(2)–Os(1)–H(2)	97	Os(3)–C(6)–O(6)	176 (1)
C(14)–Os(1)–H(1)	93	Os(3)–C(7)–O(7)	178 (1)
C(14)–Os(1)–H(2)	160	Os(3)–C(8)–O(8)	179 (1)
H(1)–Os(1)–H(2)	84	Os(3)–C(9)–C(10)	123.1 (7)
Os(3)–Os(2)–P(1)	85.60 (6)	Os(3)–C(9)–C(13)	129.9 (7)
Os(3)–Os(2)–C(3)	82.1 (3)	C(10)–C(9)–C(13)	102.7 (8)
Os(3)–Os(2)–C(4)	177.2 (3)	P(1)–C(10)–C(9)	119.2 (7)
Os(3)–Os(2)–C(5)	86.1 (3)	P(1)–C(10)–C(11)	130.7 (7)
Os(3)–Os(2)–H(1)	83	C(9)–C(10)–C(11)	110.1 (8)
P(1)–Os(2)–C(3)	91.7 (3)	C(10)–C(11)–C(12)	108.3 (8)
P(1)–Os(2)–C(4)	95.6 (3)	C(11)–C(12)–C(13)	107 (1)
P(1)–Os(2)–C(5)	170.4 (3)	C(9)–C(13)–C(12)	111.9 (8)
P(1)–Os(2)–H(1)	90	Os(1)–C(14)–C(15)	122.3 (7)
C(3)–Os(2)–C(4)	100.4 (5)	Os(1)–C(14)–C(18)	118.6 (7)
C(3)–Os(2)–C(5)	92.0 (4)	C(15)–C(14)–C(18)	105.2 (9)
C(3)–Os(2)–H(1)	164.76	C(14)–C(15)–C(16)	109 (1)
C(4)–Os(2)–C(5)	92.5 (4)	C(15)–C(16)–C(17)	109 (1)
C(4)–Os(2)–H(1)	95	C(16)–C(17)–C(18)	108 (1)
C(5)–Os(2)–H(1)	84	C(14)–C(18)–C(17)	108 (1)
Os(1)–Os(3)–Os(2)	64.82 (2)	P(1)–C(19)–C(20)	118.8 (7)
Os(1)–Os(3)–C(6)	148.2 (3)	P(1)–C(19)–C(24)	123.1 (8)
Os(1)–Os(3)–C(7)	99.0 (3)	C(20)–C(19)–C(24)	118.1 (9)
Os(1)–Os(3)–C(8)	115.9 (4)	C(19)–C(20)–C(21)	121 (1)
Os(1)–Os(3)–C(9)	60.3 (3)	C(20)–C(21)–C(22)	119 (1)
Os(1)–Os(3)–H(2)	23	C(21)–C(22)–C(23)	123 (1)
Os(2)–Os(3)–C(6)	99.9 (3)	C(22)–C(23)–C(24)	118 (1)
Os(2)–Os(3)–C(7)	163.7 (3)	C(19)–C(24)–C(23)	122 (1)
Os(2)–Os(3)–C(8)	91.0 (4)	P(1)–C(25)–C(26)	124.1 (9)
Os(2)–Os(3)–C(9)	84.1 (3)	P(1)–C(25)–C(30)	115.7 (9)
Os(2)–Os(3)–H(2)	68	C(26)–C(25)–C(30)	120 (1)
C(6)–Os(3)–C(7)	95.2 (5)	C(25)–C(26)–C(27)	120 (1)
C(6)–Os(3)–C(8)	91.0 (5)	C(26)–C(27)–C(28)	120 (1)
C(6)–Os(3)–C(9)	91.6 (4)	C(27)–C(28)–C(29)	121 (1)
C(6)–Os(3)–H(2)	167	C(28)–C(29)–C(30)	120 (1)
C(7)–Os(3)–C(8)	94.9 (5)	C(25)–C(30)–C(29)	120 (1)
C(7)–Os(3)–C(9)	89.4 (4)	Os(1)–H(1)–Os(2)	132
C(7)–Os(3)–H(2)	96	Os(1)–H(2)–Os(3)	133

Complex 4 is isolated from the products of the thermal decomposition of $Os_3(CO)_{10}[Fe(\eta\text{-}C_5H_4PPr^i{}_2)_2]$;[6] an isopropyl group is lost, probably by propene elimination following β-CH oxidative addition to an adjacent osmium center. A P–C(aryl) bond is also cleaved. There are few examples of the metal–activated cleavage of P–C(alkyl) bonds upon thermolysis,[7,8] and the stability sequence P–C(sp^3) > P–C(sp^2) > P–C(sp) is the rule.[9]

The structures of **3a** and **3b** are very similar, so metrical remarks are confined to **3b** (Figure 1). Both hydrogen atoms were located in the refinement. The Fe(1)–Os(1) length is 2.830 (1) Å, which is shorter than the Os(1)–Os(3) and Os(2)–Os(3) lengths (2.8488 (6) and 2.8876 (7) Å, respectively). The Os(1)–Os(2) distance is appreciably longer at 3.0675 (7) Å; nonetheless, there is probably a bonding interaction.[10]

---

[6] Cullen, W. R.; Rettig, S. J.; Zheng, T. C. *Organometallics*, in press.

[7] Cullen, W. R.; Rettig, S. J.; Zheng, T. C. *Organometallics*, in press.

[8] Deeming, A. J. *J. Organomet. Chem.* **1977**, *128*, 63.

[9] Garrou, P. E. *Chem. Rev.* **1985**, *85*, 171.

[10] Deeming, A. J. *Adv. Organomet. Chem.* **1986**, *26*, 1.

Table VIII. Final Atomic Coordinates (Fractional) and B_{eq} Values (Å^2)[a] for 4

atom	x	y	z	B_{eq}
Os(1)	0.30435 (4)	0.35707 (2)	0.32654 (2)	1.94 (1)
Os(2)	0.15446 (4)	0.43255 (2)	0.17490 (3)	2.41 (2)
Os(3)	0.41583 (5)	0.47113 (2)	0.29193 (3)	2.55 (2)
Fe(1)	0.1449 (1)	0.35100 (5)	0.47113 (8)	2.14 (5)
P(1)	0.3922 (3)	0.3891 (1)	0.2026 (2)	2.2 (1)
P(2)	0.2130 (3)	0.2627 (1)	0.3059 (2)	2.2 (1)
O(1)	0.6008 (8)	0.3117 (3)	0.4196 (5)	4.3 (4)
O(2)	0.219 (1)	0.5119 (3)	0.0260 (5)	6.1 (5)
O(3)	−0.069 (1)	0.5207 (4)	0.2381 (6)	7.4 (5)
O(4)	−0.043 (1)	0.3536 (3)	0.0457 (5)	5.3 (4)
O(5)	0.553 (1)	0.5517 (3)	0.1681 (6)	6.0 (5)
O(6)	0.715 (1)	0.4493 (4)	0.4084 (6)	6.7 (5)
O(7)	0.258 (1)	0.5695 (3)	0.3819 (5)	5.6 (4)
C(1)	0.485 (1)	0.3288 (4)	0.3856 (6)	2.9 (4)
C(2)	0.197 (1)	0.4822 (5)	0.0835 (7)	3.8 (5)
C(3)	0.012 (1)	0.4862 (5)	0.2149 (7)	4.6 (6)
C(4)	0.031 (1)	0.3830 (4)	0.0963 (7)	3.1 (4)
C(5)	0.501 (1)	0.5216 (4)	0.2154 (7)	3.6 (5)
C(6)	0.604 (1)	0.4600 (4)	0.3662 (8)	4.2 (5)
C(7)	0.317 (1)	0.5314 (5)	0.3512 (6)	3.6 (5)
C(8)	0.120 (1)	0.2712 (4)	0.4013 (6)	2.1 (4)
C(9)	0.188 (1)	0.2626 (4)	0.4911 (6)	2.5 (4)
C(10)	0.088 (1)	0.2837 (4)	0.5465 (6)	2.9 (4)
C(11)	−0.044 (1)	0.3055 (4)	0.4926 (6)	3.1 (5)
C(12)	−0.022 (1)	0.2996 (4)	0.4050 (6)	2.9 (4)
C(13)	0.267 (1)	0.4164 (4)	0.4208 (6)	2.5 (4)
C(14)	0.332 (1)	0.4033 (4)	0.5118 (7)	3.3 (5)
C(15)	0.220 (1)	0.4121 (4)	0.5659 (6)	2.9 (4)
C(16)	0.087 (1)	0.4315 (4)	0.5148 (7)	3.2 (4)
C(17)	0.115 (1)	0.4352 (4)	0.4278 (6)	2.6 (4)
C(18)	0.521 (1)	0.3559 (4)	0.1336 (7)	3.4 (4)
C(19)	0.678 (1)	0.3458 (5)	0.1883 (8)	5.2 (6)
C(20)	0.532 (2)	0.3938 (6)	0.0534 (8)	7.8 (8)
C(21)	0.343 (1)	0.2006 (4)	0.3318 (6)	2.5 (4)
C(22)	0.462 (1)	0.1963 (5)	0.2682 (8)	4.5 (6)
C(23)	0.272 (1)	0.1412 (4)	0.3420 (7)	4.0 (5)
C(24)	0.061 (1)	0.2445 (4)	0.2154 (6)	3.3 (4)
C(25)	−0.050 (1)	0.1967 (5)	0.2316 (8)	5.4 (7)
C(26)	0.128 (1)	0.2324 (5)	0.1306 (7)	5.3 (6)

[a] $B_{eq} = (8/3)\pi^2\sum\sum U_{ij}a_i^*a_j^*(a_i\cdot a_j)$.

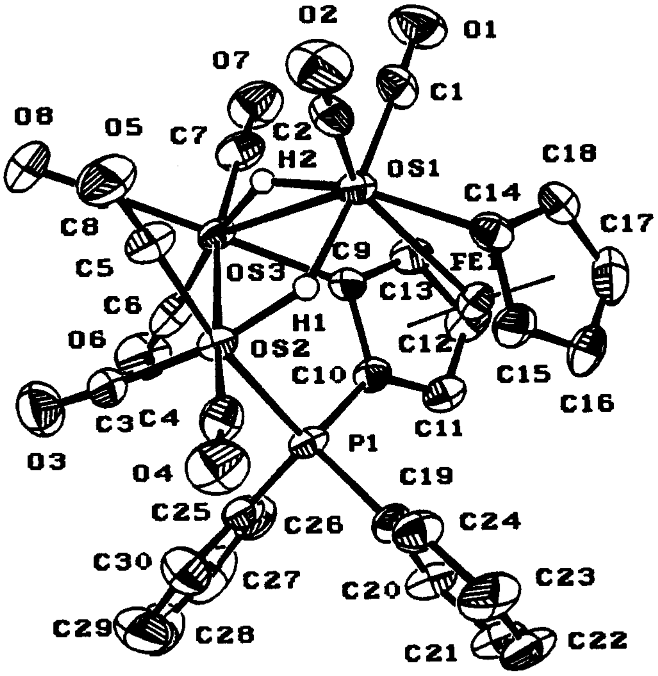

Figure 2. ORTEP plot for **3a**.

The metallocene moiety shows little distortion resulting from the Fe→Os bonding. The Fe(1)–ring centroid distances are 1.657 (3) and 1.643 (4) Å and the inter-ring plane angle is 2.24°. These data should be compared with the Fe(2)–ring centroid distances of 1.641 (3) and 1.661 (5) Å and the inter-ring–dihedral angle of 5.93°. Some motion of the iron atom toward Os(1) may be indicated by the lengthening of the Fe(1)–C(9) distance to 2.134 (5) Å and

Table IX. Bond Lengths (Å) with Estimated Standard Deviations[a] for 4

Os(1)–Os(2)	3.0513 (7)	P(1)–C(18)	1.83 (1)
Os(1)–Os(3)	2.8594 (6)	P(2)–C(8)	1.799 (8)
Os(1)–Fe(1)	2.813 (1)	P(2)–C(21)	1.83 (1)
Os(1)–P(1)	2.286 (2)	P(2)–C(24)	1.85 (1)
Os(1)–P(2)	2.305 (2)	O(1)–C(1)	1.16 (1)
Os(1)–C(1)	1.85 (1)	O(2)–C(2)	1.15 (1)
Os(1)–C(13)	2.047 (8)	O(3)–C(3)	1.16 (1)
Os(2)–Os(3)	2.8715 (9)	O(4)–C(4)	1.16 (1)
Os(2)–P(1)	2.322 (3)	O(5)–C(5)	1.15 (1)
Os(2)–C(2)	1.89 (1)	O(6)–C(6)	1.13 (1)
Os(2)–C(3)	1.92 (1)	O(7)–C(7)	1.15 (1)
Os(2)–C(4)	1.89 (1)	C(8)–C(9)	1.44 (1)
Os(3)–P(1)	2.312 (2)	C(8)–C(12)	1.43 (1)
Os(3)–C(5)	1.88 (1)	C(9)–C(10)	1.41 (1)
Os(3)–C(6)	1.90 (1)	C(10)–C(11)	1.43 (1)
Os(3)–C(7)	1.93 (1)	C(11)–C(12)	1.40 (1)
Fe(1)–C(8)	2.109 (8)	C(13)–C(14)	1.47 (1)
Fe(1)–C(9)	2.065 (9)	C(13)–C(17)	1.44 (1)
Fe(1)–C(10)	2.031 (9)	C(14)–C(15)	1.41 (1)
Fe(1)–C(11)	2.05 (1)	C(15)–C(16)	1.40 (1)
Fe(1)–C(12)	2.046 (9)	C(16)–C(17)	1.40 (1)
Fe(1)–C(13)	2.062 (9)	C(18)–C(19)	1.55 (1)
Fe(1)–C(14)	2.07 (1)	C(18)–C(20)	1.52 (1)
Fe(1)–C(15)	2.059 (9)	C(21)–C(22)	1.55 (1)
Fe(1)–C(16)	2.047 (9)	C(21)–C(23)	1.51 (1)
Fe(1)–C(17)	2.037 (8)	C(24)–C(25)	1.52 (1)
Fe(1)–Cp(1)	1.668 (4)	C(24)–C(26)	1.54 (1)
Fe(1)–Cp(2)	1.662 (4)		

[a] Here and elsewhere Cp(1) and Cp(2) refer to the unweighted centroids of the C(8–12) and C(13–17) cyclopentadienyl rings, respectively.

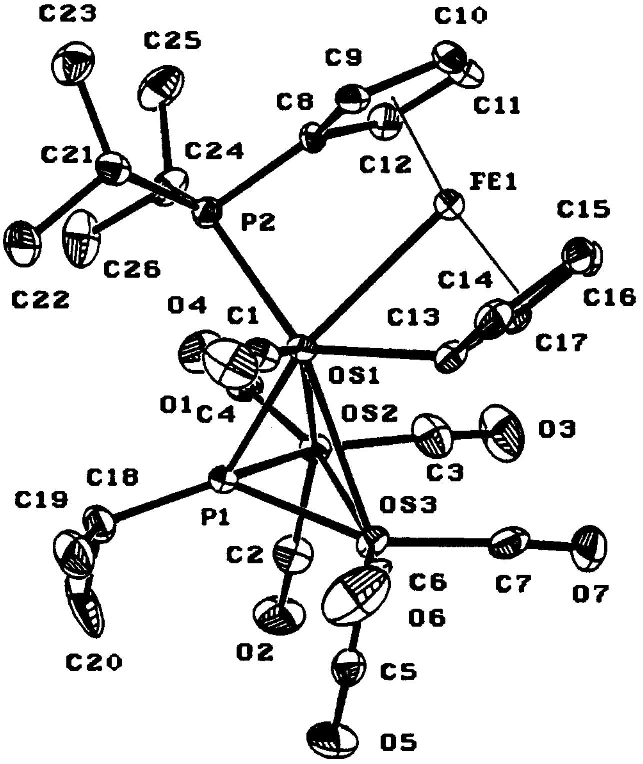

Figure 3. ORTEP plot for 4.

Table X. Bond Angles (deg) with Estimated Standard Deviations for 4

Os(2)–Os(1)–Os(3)	58.02 (2)	C(5)–Os(3)–C(6)	93.5 (5)
Os(2)–Os(1)–Fe(1)	114.80 (3)	C(5)–Os(3)–C(7)	96.5 (4)
Os(2)–Os(1)–P(1)	49.04 (6)	C(6)–Os(3)–C(7)	103.4 (5)
Os(2)–Os(1)–P(2)	108.25 (6)	Os(1)–Fe(1)–Cp(1)	106.0 (1)
Os(2)–Os(1)–C(1)	146.0 (3)	Os(1)–Fe(1)–Cp(2)	83.9 (2)
Os(2)–Os(1)–C(13)	94.2 (3)	Cp(1)–Fe(1)–Cp(2)	169.9 (2)
Os(3)–Os(1)–Fe(1)	114.90 (3)	Os(1)–P(1)–Os(2)	82.94 (8)
Os(3)–Os(1)–P(1)	51.96 (6)	Os(1)–P(1)–Os(3)	76.91 (7)
Os(3)–Os(1)–P(2)	161.32 (6)	Os(1)–P(1)–C(18)	132.1 (3)
Os(3)–Os(1)–C(1)	96.2 (3)	Os(2)–P(1)–Os(3)	76.58 (7)
Os(3)–Os(1)–C(13)	68.2 (2)	Os(2)–P(1)–C(18)	134.2 (3)
Fe(1)–Os(1)–P(1)	161.87 (7)	Os(3)–P(1)–C(18)	131.9 (3)
Fe(1)–Os(1)–P(2)	81.66 (7)	Os(1)–P(2)–C(8)	88.9 (3)
Fe(1)–Os(1)–C(1)	95.4 (3)	Os(1)–P(2)–C(21)	119.4 (3)
Fe(1)–Os(1)–C(13)	47.0 (2)	Os(1)–P(2)–C(24)	121.3 (3)
P(1)–Os(1)–P(2)	109.84 (8)	C(8)–P(2)–C(21)	104.8 (4)
P(1)–Os(1)–C(1)	98.4 (3)	C(8)–P(2)–C(24)	105.5 (4)
P(1)–Os(1)–C(13)	119.5 (2)	C(21)–P(2)–C(24)	111.2 (4)
P(2)–Os(1)–C(1)	90.4 (3)	Os(1)–C(1)–O(1)	177.1 (8)
P(2)–Os(1)–C(13)	128.6 (2)	Os(2)–C(2)–O(2)	178 (1)
C(1)–Os(1)–C(13)	95.7 (4)	Os(2)–C(3)–O(3)	177 (1)
Os(1)–Os(2)–Os(3)	57.64 (2)	Os(2)–C(4)–O(4)	177.7 (9)
Os(1)–Os(2)–P(1)	48.02 (6)	Os(3)–C(5)–O(5)	179 (1)
Os(1)–Os(2)–C(2)	142.8 (3)	Os(3)–C(6)–O(6)	175 (1)
Os(1)–Os(2)–C(3)	110.4 (3)	Os(3)–C(7)–O(7)	176 (1)
Os(1)–Os(2)–C(4)	107.8 (3)	P(2)–C(8)–C(9)	126.1 (7)
Os(3)–Os(2)–P(1)	51.56 (6)	P(2)–C(8)–C(12)	126.6 (7)
Os(3)–Os(2)–C(2)	93.0 (3)	C(9)–C(8)–C(12)	106.0 (7)
Os(3)–Os(2)–C(3)	96.7 (4)	C(8)–C(9)–C(10)	108.6 (8)
Os(3)–Os(2)–C(4)	158.6 (3)	C(9)–C(10)–C(11)	108.0 (8)
P(1)–Os(2)–C(2)	96.6 (3)	C(10)–C(11)–C(12)	107.8 (8)
P(1)–Os(2)–C(3)	146.8 (4)	C(8)–C(12)–C(11)	109.5 (8)
P(1)–Os(2)–C(4)	107.2 (3)	Os(1)–C(13)–C(14)	117.4 (6)
C(2)–Os(2)–C(3)	94.1 (5)	Os(1)–C(13)–C(17)	120.1 (7)
C(2)–Os(2)–C(4)	92.4 (4)	C(14)–C(13)–C(17)	103.7 (8)
C(3)–Os(2)–C(4)	103.6 (5)	C(13)–C(14)–C(15)	108.5 (9)
Os(1)–Os(3)–Os(2)	64.34 (1)	C(14)–C(15)–C(16)	109.3 (8)
Os(1)–Os(3)–P(1)	51.13 (6)	C(15)–C(16)–C(17)	107.7 (8)
Os(1)–Os(3)–C(5)	148.7 (3)	C(13)–C(17)–C(16)	110.8 (9)
Os(1)–Os(3)–C(6)	93.7 (3)	P(1)–C(18)–C(19)	109.7 (7)
Os(1)–Os(3)–C(7)	111.3 (3)	P(1)–C(18)–C(20)	111.0 (7)
Os(2)–Os(3)–P(1)	51.86 (6)	C(19)–C(18)–C(20)	111 (1)
Os(2)–Os(3)–C(5)	99.0 (3)	P(2)–C(21)–C(22)	112.3 (6)
Os(2)–Os(3)–C(6)	154.2 (3)	P(2)–C(21)–C(23)	117.3 (7)
Os(2)–Os(3)–C(7)	97.5 (3)	C(22)–C(21)–C(23)	110.0 (8)
P(1)–Os(3)–C(5)	97.6 (3)	P(2)–C(24)–C(25)	117.5 (8)
P(1)–Os(3)–C(6)	104.3 (3)	P(2)–C(24)–C(26)	110.5 (7)
P(1)–Os(3)–C(7)	148.0 (3)	C(25)–C(24)–C(26)	110.8 (9)

the shortening of Fe(1)–C(14) to 1.964 (6) Å. The average Fe(2)–C distance in the dangling ferrocene moiety of **3b** is 2.041 Å. The C(9)Os(3)Os(1)C(14) torsion angle is 10.3 (3)°, so the C_5 rings are slightly staggered. Os(1) is 1.2374 Å distant from the C_5 plane, almost as much as Fe(1) (1.6395 Å).

The structure of **4** (Figure 3) shows the phosphinidene group indicated by the ^{31}P NMR resonance at 268.3 ppm. There are two short Os–Os bonds (Os(2)–Os(3) = 2.8715 (9) Å and Os(1)–Os(3) = 2.8594 (6) Å); the longer Os(1)–Os(2) bond (3.0513) (7) Å) is probably bridged by the H atom that was not located in the refinement in spite of excellent data. The C(8)P(2)Os(1)C(13) torsion angle is 1.6 (5)°, so the C_5 rings are eclipsed as in **3**. The Os(1)–Fe(1) distance 2.813 (1) Å is shorter than in **3** and the C_5 rings are considerably tilted, the dihedral angle between them being 11.85°. However, this angle is less than the 21.0° measured for **1**. As in **3b**, Os(1) is not in the plane of the C_5 ring and is almost as far away from this plane (1.3415 Å) as is Fe(1) (1.6610 Å).

We have recently described ruthenium complexes that are closely related to the derivatives with Fe→Os bonds described above, although solid-state data were not obtained.[7] It seems that this chemistry involving M(metallocene fragment)→M′ (metal cluster) bonds may be quite extensive. Further work is in progress.

Acknowledgment. We thank the Natural Sciences and Engineering Research Council of Canada for support of this work.

Registry No. **3a**, 137140-11-5; **3b**, 137140-12-6; **3b**·$0.5CH_2Cl_2$, 137140-13-7; **4**, 137140-14-8; $Os_3(CO)_{10}(PFcPh_2)_2$, 137140-15-9; $Os_3(CO)_{11}PFc_2Ph$, 137140-16-0.

Supplementary Material Available: For **3a**, **3b**, and **4**, textual description of experimental procedures, stereo ORTEP diagrams, ORTEP figures with hydrogen atoms, and tables of experimental details, hydrogen positional and thermal parameters, general temperature factor expressions, torsion angles, intermolecular contacts up to 3.60 Å, and least-square planes, and, additionally for **4**, tables of intramolecular bond distances and angles (61 pages); listings of observed and calculated structure factor amplitudes for **3a**, **3b**, and **4** (191 pages). Ordering information is given on any current masthead page.